International Conference on Nuclear Data for Science and Technology 2007
DOI: 10.1051/ndata:07285

Invited

ENDF/B-VII data testing with ICSBEP benchmarks

A.C. Kahler and R.E. MacFarlane

Los Alamos National Laboratory, Los Alamos, NM, USA

Abstract. Continuous energy Monte Carlo eigenvalue calculations have been performed for several hundred critical benchmarks described in the International Handbook of Evaluated Criticality Safety Benchmark Experiments. These calculations were performed with MCNP5 using either ENDF/B-VI.8 or ENDF/B-VII.0 cross sections. ENDF/B-VII cross section data files yield significantly more accurate calculated eigenvalues than those obtained with ENDF/B-VI.8 cross sections for moderated, low-enriched uranium fuel rod lattice configurations and for unmoderated, bare or reflected, critical benchmark assemblies. Accurate calculated eigenvalues were previously obtained with ENDF/B-VI.8 cross sections for both highly-enriched and low-enriched uranium solution assemblies. These accurate eigenvalues are retained with ENDF/B-VII.0 cross sections.

1 Introduction

The ENDF/B-VII.0 cross section library, ref. [1], was released in December 2006. We have performed continuous energy Monte Carlo eigenvalue calculations using the MCNP5, ref. [2], code coupled with ENDF/B-VI.8 ref. [3] and ENDF/B-VII.0 cross sections for a variety of critical benchmarks defined by the International Criticality Safety Benchmark Evaluation Project (ICSBEP) in the International Handbook of Evaluated Criticality Safety Benchmark Experiments, ref. [4]. Comparison of calculated eigenvalues from these different neutron cross section libraries demonstrates that the new cross section data files yield significantly more accurate calculated eigenvalues for a wide range of critical systems, whether moderated or unmoderated and whether bare, water reflected or reflected by non-hydrogenous materials.

2 Discussion

Results of our Monte Carlo eigenvalue calculations are presented below. We initially describe the processing of these cross sections into suitable input files for MCNP, then compare and contrast the ENDF/B-VI.8 based and ENDF/BVII.0 based calculated eigenvalues. These results are generally grouped by fissile system and/or degree of moderation, using standard ICSBEP definitions.

2.1 Cross section processing with NJOY and MCNP running strategy

ENDF/B-VI.8 based continuous energy neutron cross section files have long been available for MCNP users, ref. [5]. The ENDF/B-VI.8 eigenvalue results presented in this paper use these publicly available files. The NJOY Nuclear Data Processing System, ref. [6], has been used to process ENDF/B-VII.0 neutron files into the ACE format required by MCNP. Pointwise, linearly interpolable cross sections have been generated and Doppler broadened to a temperature of 293.6°K with a reconstruction tolerance of 0.1%. In addition, NJOY's PURR module was used to generate unresolved resonance probability tables for those evaluations that contain unresolved resonance parameters. A generic input deck was used that created 20 probability bins with 32 resonance ladders per bin for all such nuclides. The THERMR module was used to generate room temperature thermal scattering kernels.

Single processor and MPI versions of MCNP5 have both been utilized to perform the calculations reported below. A typical job tracks 25 to 50 million neutron histories, resulting in a calculated eigenvalue uncertainty that is typically less than 25 pcm, and frequently near 10 pcm. Typically the first 50 cycles are discarded in these jobs. Single processor jobs generally execute 10,000 histories for 5000 active cycles; multi-processor jobs typically execute 20,000 to 50,000 histories per active cycle. When run to such precision, stochastic fluctuations in the calculated eigenvalue are minimal and so C/E eigenvalue deviations from unity are not a consequence of random fluctuation. Because of the small calculated eigenvalue uncertainty, we do not show these error bars in the figures that follow.

2.2 Results for traditional unmoderated LANL benchmarks

Traditional Los Alamos National Laboratory (LANL) benchmarks include bare cores of highly-enriched uranium (Godiva, HEU-MET-FAST-001), ^{239}Pu (Jezebel, PU-MET-FAST-001 and Jezebel-240, PU-MET-FAST-002) or ^{233}U (Jezebel-23, U233-MET-FAST-001). Reflected versions of these cores include HEU-MET-FAST-028 (Flattop-25), PU-MET-FAST-006 (Flattop-Pu), PU-MET-FAST-008 (Thor) and U233-MET-FAST-006 (Flattop-23). The "Flattop" cores include a natural uranium reflector while "Thor" has a ^{232}Th reflector. Also shown is the heterogeneous Big-10 (IEU-MET-FAST-007) core.

Eigenvalues, calculated with both ENDF/B-VI.8 and ENDF/B-VII.0 cross sections are shown in figure 1. The "open" data points are ENDF/B-VI.8 based results; the "closed" data points illustrate calculated eigenvalues using ENDF/B-VII.0 cross sections. Error bars, centered on unity, illustrate the estimated experimental uncertainty.

Article available at http://nd2007.edpsciences.org or http://dx.doi.org/10.1051/ndata:07285

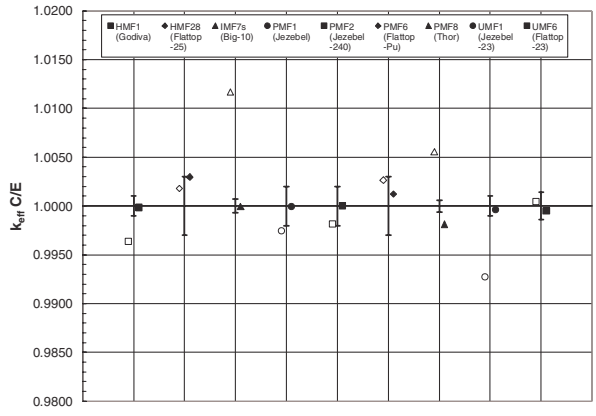

Fig. 1. Calculated eigenvalues using ENDF/B-VII.8 cross sections and ENDF/B-VII.0 cross sections for "traditional" LANL unmoderated benchmarks.

The ENDF/B-VI.8 based calculated eigenvalues exhibit two deficiencies that are largely corrected with ENDF/B-VII.0 cross sections. First, the bare HEU, Pu and ^{233}U configurations exhibit a systematic bias of several hundred pcm in calculated eigenvalue – $\sim$−350 pcm for Godiva, $\sim$−250 pcm for Jezebel and $\sim$−700 pcm for Jezebel-23. Secondly, this eigenvalue bias shifts by more than 500 pcm when ^{nat}U or Th reflectors are added. The Big-10 benchmark has a large positive (over 1000 pcm) calculated eigenvalue bias.

These biases are virtually eliminated when ENDF/B-VII.0 cross sections are used. The bare system eigenvalues range from a low of 0.99960(8) for Jezebel-23 to a high of 1.00000(8) for Jezebel-240 (where the value appearing in parentheses is the MCNP uncertainty on the calculated eigenvalue). The Flattop-Godiva reflector bias is reduced to $\sim$300 pcm while it is less than 200 pcm for the Pu systems and virtually zero for the ^{233}U system; results that are significantly improved in all cases for ENDF/B-VII.0 versus ENDF/B-VI.8. The improvement is particularly noticeable for Big-10. Changes in the ^{238}U inelastic scattering secondary distributions and the elastic scattering angular distributions are believed to be the primary cause of this improvement. These cross section changes are also responsible for a significant improvement in calculated eigenvalues for low-enriched uranium lattice system that are representative of commercial fuel systems. These results are presented below, in section 2.5.

2.3 Results for other unmoderated benchmarks

In addition to the LANL benchmarks described above, a number of ICSBEP unmoderated benchmarks exist that define either a bare system or a similar system with various reflectors. Examples include HEU-MET-FAST-008 (or -015 or -065), bare HEU spheres or cylinders and HEU-MET-FAST-011 or -020 (a polyethylene reflector), -019 (a graphite reflector), -012 or -022 (an aluminum alloy reflector), -013 or -021 (a steel) reflector, -014 or -029 (a depleted uranium reflector), or -027 (a lead reflector). Other benchmarks include interleaved polyethylene plates among the HEU plates and may then include polyethylene or metallic axial and radial reflectors. Similar examples can also be found in the PU-MET-FAST benchmark category. Our calculations for some of these benchmarks, summarized in table 1, generally show a positive bias in calculated eigenvalue when a reflector is present.

Table 1. Calculated eigenvalues for unmoderated systems with various reflectors.

ICSBEP Benchmark	Reflector	Average ENDF/B-VI.8 Calculated Eigenvalue	Average ENDF/B-VII.0 Calculated Eigenvalue
HMF-008		0.9934(1)	0.9970(1)
HMF-015	(None)	0.9918(1)	0.9951(1)
HMF-065		0.9954(1)	0.9986(1)
HMF-011		- - -	1.0003(1)
	Polyethylene		
HMF-020		0.9969(1)	1.0009(1)
HMF-019	Graphite	1.0032(1)	1.0071(1)
HMF-012		- - -	0.9991(1)
HMF-022	Aluminum	0.9926(1)	0.9977(1)
HMF-013		- - -	0.9939(1)
HMF-021	Steel	0.9984(1)	0.9975(1)
HMF-027	Lead	1.0057(1)	1.0007(1)
HMF-014	Depleted	- - -	0.9988(1)
HMF-029	uranium	1.0024(1)	1.0057(1)
PMF-022		0.9960(1)	0.9985(1)
PMF-029	(None)	0.9933(1)	0.9956(1)
PMF-024		0.9996(1)	1.0019(1)
PMF-031	Polyethylene	1.0022(1)	1.0044(1)
PMF-023		0.9977(1)	0.9999(1)
PMF-030	Graphite	1.0010(1)	1.0028(1)
PMF-025		0.9965(1)	0.9989(1)
PMF-026		0.9967(1)	0.9985(1)
PMF-028	Steel	0.9975(1)	0.9991(1)
PMF-032		0.9969(1)	0.9985(1)
PMF-035	Lead	1.0080(1)	0.9978(1)

These calculated eigenvalues are not as close to unity as those presented previously; results that will require further investigation. Nevertheless, there are clear examples of improved reactivity predictions in this table. For example, the lead reflected eigenvalues were more than 1% greater than the corresponding bare HEU or Pu core when calculated with ENDB/B-VI.8 cross sections. However, with ENDF/BVII.0 cross sections, this bias decreases to about 0.2%. The cross section evaluations for other materials, such as graphite, aluminium or steel (composed primarily of iron, but also containing chromium and nickel) have changed little or not

at all between ENDF/B-VI.8 and ENDF/B-VII.0 and this is reflected in their calculated eigenvalues where the increased calculated eigenvalue is largely due to the changed actinide cross sections of the underlying core.

Calculated eigenvalues for other unmoderated benchmarks exhibit mixed results. For example, the beryllium reflected HEU-MET-FAST-041 and -058 benchmarks appear to display a clear increasing eigenvalue trend with ENDF/B-VI.8 cross sections; a trend that is virtually eliminated when ENDF/B-VII.0 eigenvalues are calculated. At the same time however, the beryllium reflected HEU-MET-FAST-066 and -077 benchmarks are accurately calculated with ENDF/B-VI.8 cross sections and are biased low by nearly 0.5% with ENDF/B-VII.0 cross sections. Similarly, the calculated eigenvalues for the titanium reflected HEU-MET-FAST-079 benchmark are tightly clustered near 0.995 when ENDF/B-VI.8 cross sections are used, but exhibit a clear increasing eigenvalue trend with reflector thickness, increasing from 1.0015(9) to 1.0054(9), when ENDF/B-VII.0 cross sections are employed. This, despite that fact that ENDF/B-VI.8 uses an elemental evaluation originally developed in the late 1970s for ENDF/B-V while ENDF/B-VII.0 has adopted the recent JENDL isotopic cross section evaluation.

2.4 Results for HEU and low-enriched solution systems

Calculated eigenvalues for HEU solution systems is an ENDF/B-VI success story. We have performed calculations for 42 HEU critical solution systems defined in 11 HEU-SOL-THERM (HST1, 9, 10, 11, 12, 13, 32, 42, 43 and 50) benchmarks. The borated HST13 configurations are omitted in this analysis. Among these benchmarks are water reflected and unreflected systems. For this class of benchmark, calculated eigenvalues have traditionally been correlated versus Above-Thermal Leakage Fraction (ATLF). Geometrically large systems exhibit minimal leakage and have ATLF values that are typically less than 0.1. Smaller systems, whether bare or reflected, exhibit leakage fractions that can exceed 0.5. Calculated eigenvalues are related to ATLF through a simple linear correlation, $k_{calc}(ATLF) = c_0 + c_1 * ATLF$. In an ideal situation the intercept term, c_0, will be unity – indicating no bias – and the slope, c_1, will be zero – indicating no trend – in calculated eigenvalues. Deviations from these values indicate a deficiency in some aspect of the input data; usually in the basic nuclear data. For ENDF/BVI.8, the c_0 and c_1 regression coefficients were determined to be 1.0009(31) and -0.0020(83), respectively (where the values in parentheses are 95% confidence intervals on the preceding coefficient). These results, an intercept term that is statistically equivalent to unity and a slope term that is statistically equivalent to zero demonstrate the high accuracy with which the critical eigenvalue can be calculated for these systems. Obviously, a goal in the development of ENDF/B-VII was to retain these excellent results while simultaneously reducing other deficiencies.

The results displayed in figure 2 demonstrate that this goal has been achieved. The individual calculated eigenvalues are shown with the various symbols as defined in the Legend.

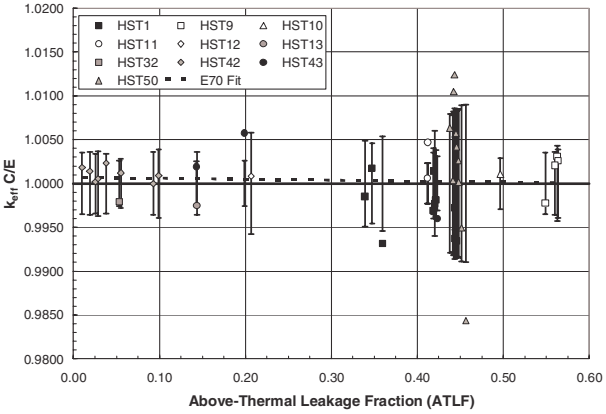

Fig. 2. Calculated eigenvalues with ENDF/B-VII.0 cross sections for a selection of HEU-SOL-THERM benchmarks.

The error bars illustrate the experimental uncertainty and the linear regression, labelled "E70 fit" is given by the dotted line. The ENDF/B-VII.0 c_0 and c_1 regression coefficients are 1.0007(32) and -0.0011(84), respectively. As with ENDF/B-VI.8 cross sections, the intercept term remains statistically equivalent to unity and the slope is statistically equivalent to zero.

In addition to HEU solutions, we have calculated critical eigenvalues for a selection of LEU solutions – 20 configurations from the LEU-SOL-THERM-004, -007, -020 and -021 benchmarks. These benchmarks have not been included in the regression analysis, but with calculated eigenvalues that are individually within 200 pcm of unity (and with a collective average of 1.00019) for ATLF values of ~0.1 to ~0.2, their eigenvalues are well predicted by the ATLF regression defined above. The average ENDF/B-VII.0 calculated eigenvalue for the complete suite of 62 solution benchmarks is 1.00029, with a 50 pcm standard deviation on the average and a 394 pcm standard deviation for the population.

2.5 Results for low-enriched UO_2 lattice systems

Calculated eigenvalues for low enriched lattice systems have a long history of being under-predicted. Until ENDF/B-VII, typical eigenvalues for this class of critical system were up to 1000 pcm too low; results that have in the past lead to ad hoc changes in cross sections, primarily for low energy ^{238}U capture, by the commercial thermal reactor design community. We have calculated a number of the ICSBEP LEU-COMP-THERM benchmarks, including LCT1 (8 cases), LCT2 (up to 5 cases), LCT6 (18 cases), LCT7 (10 cases), LCT22 (7 cases), LCT24 (2 cases) and LCT39 (up to 10 cases) with both ENDF/B-VI.8 and ENDF/B-VII.0 cross sections. This suite of benchmarks cover a range of enrichments from a low of ~2.35 wt.% ^{235}U to a high near 10 wt.% and represent experimental results from Laboratories around the world – the United States for LCT1 & -2, Japan for LCT6, France for LCT7 & -39 and Russia for LCT22 & -24. The average eigenvalue for each of these benchmarks is summarized in table 2.

There are a number of observations to make concerning the data in table 2. For example, the ENDF/B-VI.8 cross

Table 2. Calculated eigenvalues for LEU-COMP-THERM benchmarks with ENDF/B-VI.8 and ENDF/B-VII.0 cross sections.

LEU-COMP-THERM-### Benchmark	Average ENDF/B-VI.8 Calculated Eigenvalue	Average ENDF/B-VII.0 Calculated Eigenvalue
−001	0.9935(10)	0.9989(9)
−002	0.9926(11)	0.9992(7)
−006	0.9934(7)	1.0000(3)
−007	0.9935(22)	0.9984(6)
−022	1.0014(31)	1.0049(26)
−024	0.9993(68)	1.0049(50)
−039	0.9912(9)	0.9974(5)
Combined results	0.9943(34)	0.9996(26)

section results demonstrate the historical trend of under-predicting the calculated critical eigenvalue for these systems. The number in parenthesis is the standard deviation associated with the population that produced that average eigenvalue. Small values, such as determined from the individual cases that comprise the LCT6 benchmark indicate that similar calculated eigenvalues are obtained for all cases of this benchmark, while large values such as obtained in the LCT24 calculations indicate a large spread in the individual eigenvalues. In the case of LCT22 and LCT24, which do not conform to the historical pattern of too low a calculated eigenvalue, there is almost a 1000 pcm spread in the individual calculated eigenvalues.

In recent years, there has been a renewed focus on the issue of under-predicted reactivity in LEU systems, culminating in an NEA sponsored international collaboration, ref. [7], that has successfully resolved this issue. This is illustrated by the data in the ENDB/B-VII.0 column of table 2, where significant increases in calculated eigenvalues are observed. These increases generally serve to move the calculated eigenvalues closer to unity, and perhaps more importantly, the standard deviation for a majority of these benchmarks is now smaller. This result indicates that not only has the absolute accuracy in the calculated eigenvalue improved, but that underlying trends, such as a drift in calculated eigenvalue as a function of ^{238}U absorption fraction, have also been reduce or eliminated. This general observation applies to both the individual benchmark results as well as to the combined results. Another measure of the improvement in these calculated eigenvalues is that the smallest ENDF/BVI.8 calculated eigenvalue was 0.9899(1), for LCT39, case 4, whereas with ENDF/B-VII.0 cross sections, this calculated eigenvalue increases to 0.9965(1).

2.6 Results for Pu solution systems

Critical eigenvalues have been calculated with ENDF/B-VI.8 and ENDF/B-VII.0 cross sections for a suite of 117 critical configurations defined in 15 PU-SOL-THERM benchmarks (PU-SOL-THERM-001, -002, -003, -004, -005, -006, -007, -009, -010, -011, -012, -018, -022, -028 & -032). As noted in ref. [1], there has been little work to improve thermal plutonium cross sections in recent years. ENDF/B-VII.0's thermal plutonium cross sections are largely carried over from ENDF/B-VI.8, and therefore the differences in calculated eigenvalues are small and largely reflect modest changes in oxygen cross sections, hydrogen bound in water thermal scattering and in the thermal Pu fission spectrum. Our results are summarized in table 3.

Table 3. Calculated Eigenvalue Summary for PU-SOL-THERM Benchmarks with ENDF/B-VI.8 and ENDF/B-VII.0 cross sections.

	ENDF/B-VI.8	ENDF/B-VII.0
Average eigenvalue & uncertainty	1.0039 ± 0.0004 (average) ± 0.0043 (population)	1.0048 ± 0.0004 (average) ± 0.0044 (population)
Minimum Eigenvalue	0.9941(11)	0.9936(11)
Maximum Eigenvalue	1.0194(5)	1.0195(6)

We have attempted to correlate these eigenvalues against a variety of system parameters, such as ^{240}Pu atom fraction, ^{241}Pu production fraction, hydrogen absorption, average fission energy or ATLF, but have yet to discover a unique regression parameter that can explain the systematic deviation from unity observed in these calculated eigenvalues. Clearly this is an area where additional experimental and evaluation work is needed.

2.7 Results for ^{233}U solution systems

The ICSBEP Handbook describes a number of ^{233}U fluoride critical solution experiments. Eight of these evaluations (U233-SOL-THERM-001, -005, -008, -009, -012, -013, -016 and -017) encompassing over 70 critical configurations define bare or water reflected systems. Calculated eigenvalues have been correlated with ATLF, as was done for the HST and LST systems described earlier. With ENDF/B-VI.8 cross sections the c_0 and c_1 regression coefficients are 0.9974(39) and +0.0123(88), respectively. Unfortunately, these systems are not distributed as uniformly in the ATLF space as were the HST systems. The large uncertainty on the intercept term, c_0, is caused by a lack of data for small ATLF values. Of the 74 critical systems analyzed, only five have ATLF values less than 0.1. ENDF/B-VII.0 ^{233}U has a larger thermal ν than ENDF/BVI.8 plus a somewhat harder fission spectrum. These changes yield ENDF/B-VII.0 c_0 and c_1 regression coefficients of 1.0005(33) and +0.0074(75), respectively. Although few in number, the low ATLF value configurations are the most important configurations for confirming the accuracy of thermal cross section data. It is gratifying then to see the c_0 (intercept) term move significantly closer to unity when ENDF/B-VII.0 cross sections are employed. However, the magnitude of the regression slope remains disturbingly large, suggesting that further improvements, perhaps in the higher energy cross sections or fission spectrum, are needed.

Two other ^{233}U fluoride solution evaluations defined in the Handbook (U233-SOL-INTER-001 and U233-SOL-THERM-015) describe critical systems reflected by Be, polyethylene (or both). Calculations for 54 of these configurations are uniformly low, by as much as 3%, regardless of cross section library. These systems have much larger above-thermal fission fractions than observed in the bare and water reflected U233-SOL experiments, suggesting that significant nuclear data deficiencies remain in the above-thermal energy region.

3 Conclusions

Hundreds of critical experiments defined in the ICSBEP Handbook have been calculated using continuous energy Monte Carlo with ENDF/B-VI.8 and ENDF/B-VII.0 cross sections. These critical systems have included one or more of ^{233,235,238}U and ^{239}Pu under moderated and unmoderated conditions. Moderators include water, polyethylene, beryllium and beryllium-oxide. A variety of reflector materials are also present in these experiments, including water, beryllium, aluminium, titanium, steel (primarily iron), nickel and lead. In many instances, ENDF/B-VII.0 based calculated eigenvalues are more accurate than those obtained using ENDF/B-VI.8 cross sections. This is particularly true for the traditional LANL fast critical experiments and for the long under-predicted LEU-COM-THERM class of problems representative of commercial reactors.

This work was carried out under the auspices of the National Nuclear Security Administration of the US Department of Energy at Los Alamos National Laboratory under Contract No. DE-AC52-06NA25396.

References

1. M.B. Chadwick et al., Nucl. Data Sheets **107**, 2931 (2006).
2. X-5 Monte Carlo Team, *MCNP – A General Monte Carlo NParticle Transport Code, Version 5, Volume 1: Overview and Theory,* LA-UR-03-1987, April 2003.
3. V. McLane et al., *ENDF/B-VI Summary Documentation, Supplement 1*, BNL-NCS-17541 (ENDF-201), December 1996.
4. J. Blair Briggs (ed.), *International Handbook of Evaluated Criticality Safety Benchmark Experiments,* NEA/NSC/ DOC(95)03 (the 2005 or 2006 editions of the Handbook were used to create the MCNP models for benchmarks noted in this paper).
5. MCNP5DATA: Standard Neutron, Photoatomic, Photonuclear, and Electron Data Libraries for MCNP5. Distributed with the MCNP5 code by the Oak Ridge Radiation Shielding Information Computer Center as CCC-710, or as a stand-alone data package, DLC-200.
6. R.E. MacFarlane, D.W. Muir, *The NJOY Nuclear Data Processing System, Version 91,* LA-12740-M, October 1994.
7. A. Courcelle (coordinator), R.D. McKnight (monitor), *International Evaluation Cooperation, Volume 22, Nuclear Data for Improved LEU-LWR Reactivity Predictions,* NEA/WPEC-22, OECD 2006 (NEA No. 6199).